VOL. 17, NO. 2, MARCH-APRIL 1980 J. SPACECRAFT 145
ARTICLE NO. 80-4026

The Geostationary Radiation Environment

E. G. Stassinopoulos*
NASA Goddard Space Flight Center, Greenbelt, Md.

A study of the geostationary radiation environment is presented. The distribution of charged particles is reviewed in terms of population domains, where trapped constituents (energetic electrons and protons) and transients (solar flare protons) have been considered. Synchronous geomagnetic geometry is discussed, and temporal and spatial variations of trapped particles are briefly reviewed. A short description of the current standard environment models is given. Probabilistic solar flare proton predictions are described, including the distinction between ordinary event and anomalously large event fluences and the probability of occurrence of anomalously large events. A special solar proton evaluation approach is suggested for extended manned missions in the synchronous altitude regime. Finally, calculational results are presented for orbital flux integrations and dose and shielding evaluations. The data, given in graphic and tabular form, are explained and discussed.

Introduction

SINCE the early days of spaceflight, the ambient radiation has been of concern to every project manager, spacecraft designer, and scientific experimenter because it causes: 1) serious hazard for humans, 2) degrading and damaging effects on materials, 3) saturation of instruments, and 4) interference with scientific measurements and observations. Of particular interest is the environment at synchronous altitudes. Many important missions are flying there already and others will be launched into that region during the upcoming decade 1980-1990, as for example: ESA-GEOS, GOES, ATS, IUE, TDRSS, MMS, SPS, and SMS.

The purpose of this paper is to review briefly some aspects of the synchronous environment and to discuss some preliminary results obtained for geostationary missions.

Charged Particle Domains in the Magnetosphere

Quantitative models of magnetospheric processes involving fields and particles are commonly used to evaluate the radiation exposure of geocentric missions. Such models are continually being constructed, with different degrees of sophistication, for each significant particle species populating or visiting the magnetosphere. These models describe particles in a particular volume of space. This approach is illustrated in Fig. 1, where magnetospheric space has been divided into five distinct regions, using the magnetic shell parameter L as a label.[1] Numerically, L is the approximate geocentric distance, in Earth radii, of a field line's equatorial intersect. Note however, that the geometric interpretation of L becomes increasingly invalid for equatorial distances greater than 4 Earth radii because of the more complex particle motion in the real geomagnetic field which is distorted by the solar wind interaction effects. An arrangement corresponding to that but in polar R-Λ space is also shown in Fig. 1. The dipole fieldline equation ($R = L\cos^2\Lambda$) is used to map the domains, where R is the radial distance and Λ is the invariant latitude.

The indicated domain boundaries in either notation should be considered only approximate transition areas, not actual lines. These boundaries are assumed for modeling purposes and, additionally, are used here to convey a qualitative picture of the charged particle distribution. Respective "real" boundaries are diffuse areas fluctuating in their L position due to several factors, such as magnetic perturbations (storm and substorm effects), local time effects (diurnal variation), solar cycle variation (minimum and maximum activity phases), individual solar events, etc., and, furthermore, vary with particle energy. The synchronous altitude (about 6.6 Earth radii) is indicated in both drawings by an arrow.

Energetic Van Allen belt electrons are distinguished into "inner zone" and "outer zone" populations, occupying, respectively, regions 1 and 2-3-4 and current electron models reflect this division. The $L = 2.8$ line is being used to separate the inner and outer zone domains, while the termination of the outer zone at $L = 12$ Earth radii is intended only to delineate the maximum outward extent of stable or pseudo electron trapping.

Energetic Van Allen belt protons ($E \gtrsim 6$MeV) are usually contained within a dipole shell of about $L = 4$ Earth radii. The precise volume occupied by these particles depends inversely on their energy and consequently cannot be assigned to inner and outer zones. Shown in Fig. 1 are protons with energies $E > 5$ MeV populating regions 1 and 2, with an approximate trapping domain boundary placed at $L = 3.8$ Earth radii.

Finally, the solar flare proton domain is shown in Fig. 1 to extend over regions 4 and 5. These assignments were made by assuming that particles of all energies above 10 MeV have free access to a geomagnetic cutoff latitude of 63 deg, which corresponds to an L value of about 5 Earth radii.

Synchronous Geomagnetic Geometry

The positions on a great circle in the geographic equator at synchronous altitude form the locus of the geostationary orbits. However, in a magnetic reference frame, particularly in the B-L coordinate system, where B is the magnitude of the field at a given location, all such points are not equivalent. For example, in the simplest approximation to reality, the geomagnetic coordinate system (Fig. 2), which assumes an inclined and centered dipole field, the synchronous great circle has only two points that lie on the geomagnetic equator—at the nodes of intersection of the two equatorial planes. All other points lie on dipole field lines that intersect the geomagnetic equator at distances greater than the synchronous altitude. Thus, if the synchronous great circle were geomagnetically mapped in terms of L vs longitude, where L would be calculated from the centered dipole field only, it would form a typical periodic curve of two cycles. But since the actual internal-source field is neither a dipole nor is it

Received Jan. 31, 1979; revision received June 26, 1979. This paper is declared a work of the U.S. Government and therefore is in the public domain. Reprints of this article may be ordered from AIAA Special Publications, 1290 Avenue of the Americas, New York, N.Y. 10019. Order by Article No. at top of page. Member price $2.00 each, nonmember, $3.00 each. **Remittance must accompany order.**

Index categories: Atmospheric and Space Sciences; Earth-Orbital Trajectories; Meteoroid and Radiation Protection.

*Physicist, National Space Science Data Center.

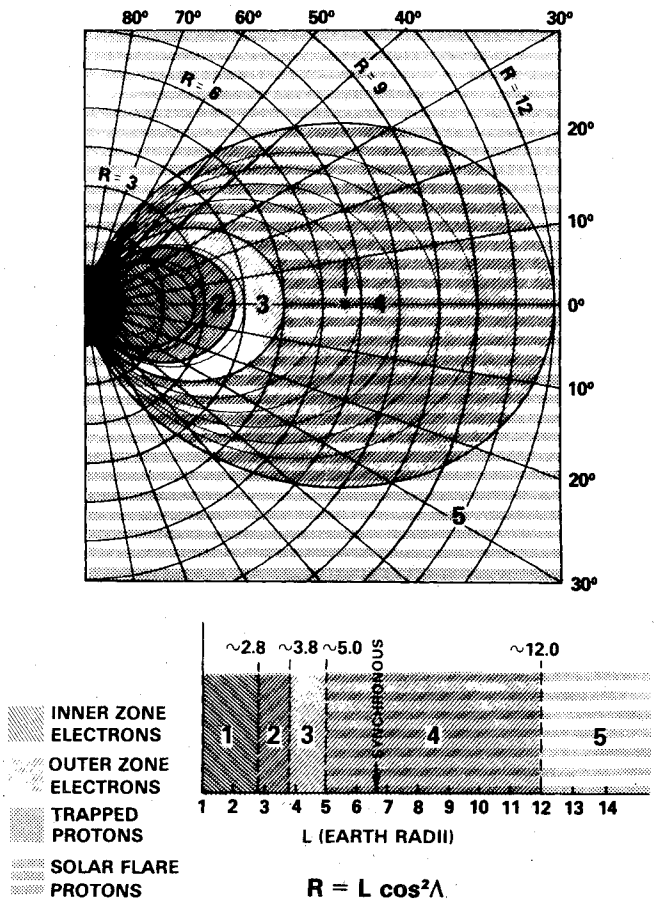

Fig. 1 Charged particle distribution in the magnetosphere.

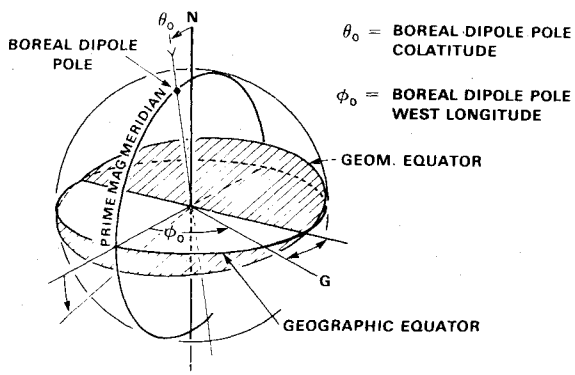

Fig. 2 Geomagnetic coordinate system.

centered, resembling rather an eccentric and displaced multipole, a truer mapping of the geostationary locus would look like the curve shown in Fig. 3. The term "truer" is used because not even this curve is absolutely correct. A more realistic representation would have to include external field contributions from electric fields, currents, etc., caused by the interaction of the solar wind with the magnetosphere, and would have to consider resulting diurnal variations (local time effects). The azimuthal asymmetry displayed by the L trace in Fig. 3 is an indication of the main field's eccentric configuration.

Variations of Geostationary Electron Environment

L Dependence

It is immediately apparent from an inspection of Fig. 3 that the geostationary satellites may have different L values associated with their parking longitude position (from 6.60 to

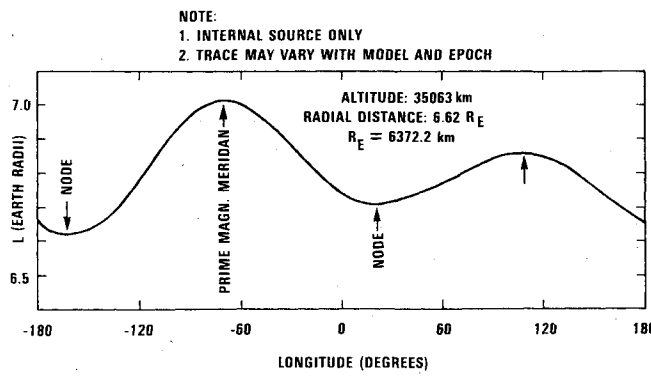

Fig. 3 L trace of the geostationary equator.

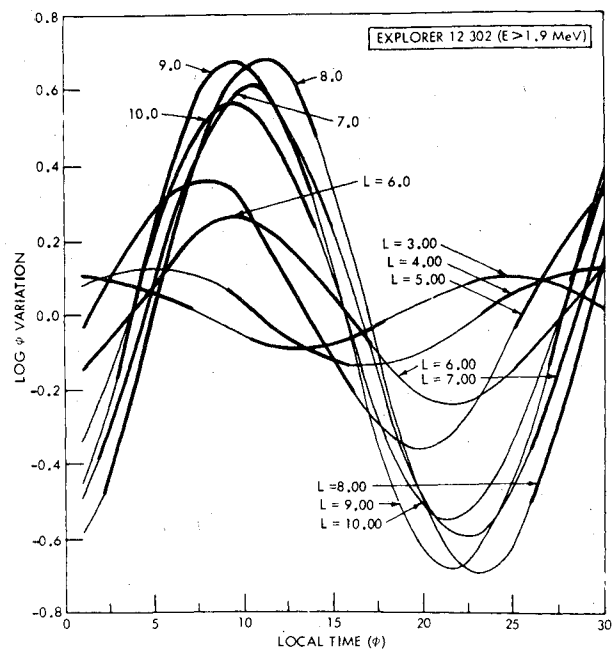

Fig. 4 Outer zone electrons: local time variations.

7.02 Earth radii). This in turn implies different radiation level and spectral distribution predictions because of the strong radial dependence of the time-averaged trapped electron population, as expressed by model environments which use the B-L internal field coordinate system.

Local Time (LT) Dependence

The average diurnal variation of electron fluxes will be different over this L range. An example is shown in Fig. 4 for electrons with energies E greater than 1.9 MeV.[2] At this energy, the maximum flux variation between extrema, expressed as the ratio of the highest to the lowest value, is about a factor of 6 and 16, respectively, at the geostationary L range limits of 6.6 and 7.0 Earth radii. For these limits, the extrema occur at corresponding local times of about 10 and 11 h for the high, and of about 22 and 23 h for the low. However, ratios and times of extrema occurrence are functions of energy E, parameter L, and, to a very small degree, epochs in solar cycles 19 and 20. As for the last effect, the LT dependence on the trapped electron population is slightly greater at solar minimum than at solar maximum because the population is believed to have been raised ("pumped up") to somewhat higher levels during the active phase of the solar cycle 20.

Temporal Dependence

Finally, at synchronous altitudes the electron population experiences strong short-term temporal variations. These are

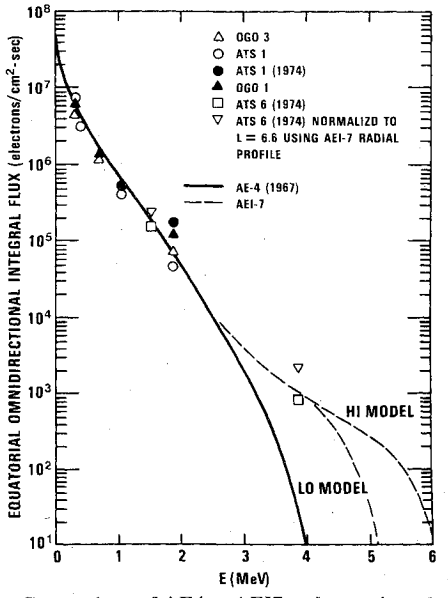

Fig. 5 Comparison of AE4 to AEI7 and to various data sets.

large substorm induced changes in the flux levels, when energetic electrons may experience a 2-3 order of magnitude rise in hours to days, and a corresponding decay in days. No significant long-term or solar cycle variations occur at geostationary altitudes. The quantitatively important effects of such variations, where fluxes may vary by about a factor of 2-4 (depending upon E and L) between average solar minimum and solar maximum values, are not apparent above $L = 5$ Earth radii based on data obtained from 1964 to 1977.

Outer Zone Electron Models

An interim outer zone electron model, AEI-7 was recently released,[3] to account for some discrepancies between AE4[4] and some newer radiation data in high gradient regions of E, B, and R. However, this interim model does not reflect the outer zone secular variations of AEI4 attributed to solar cycle effects. The final AEI7 model will account for these secular variations. This interim model was issued in two versions, the AEI7-HI and the AEI7-LO, because for energies above 1.5 MeV, it contains upper and lower limit values to account for the discrepancy between existing data sets which require further analysis to resolve. The AEI7 substantially improves high energy predictions, which were too benign in AE4 (there were insufficient high energy data available at the time of its construction).

Figure 5 shows a comparison of the AE4 to the AEI7 and to various satellite data for $L = 6.6$ Earth radii.[5] It is important to note that below about $E = 2$ MeV, the two models give virtually the same time-averaged flux levels.

Trapped Proton Models

In 1976 a single trapped proton model, the AP8,[6] replaced several older models (e.g., AP5, AP6, AP7)[7-9] each of which was valid only over a specific energy range. The new AP8 describes the entire energy spectrum in a coherent, uniform, and continuous way. It was issued in two versions: the AP8-MAX and the AP8-MIN relating, respectively, to average solar maximum and solar minimum conditions. In this case there is a good theoretical reasoning for solar cycle effects which have been verified by experimental observations. Trapped protons are affected by solar cycle variations only in the vicinity of the atmospheric cutoff regions. No changes of consequence have been observed in the heart of the proton trapping domain or at synchronous altitudes since the observed temporal variations are in most cases of no greater extremes than the precision obtained between measurements by detectors on different satellites.

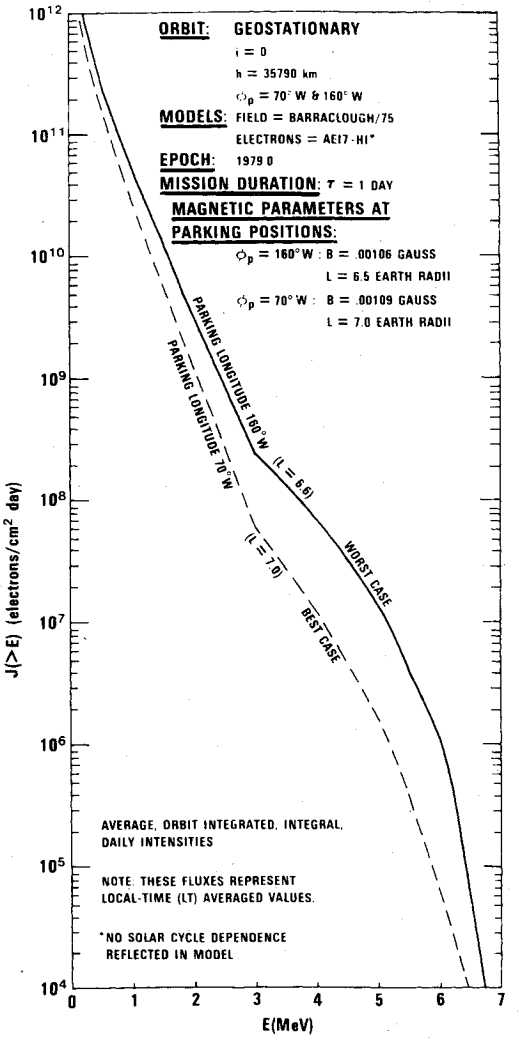

Fig. 6 Outer zone electron fluxes.

Solar Flare Protons

Synchronous orbits do not experience any significant amount of geomagnetic shielding for cosmic rays of solar or galactic origin in the energy range $E > 10$ MeV. Therefore, it may be assumed that geostationary spacecraft will be 100% exposed to the unattenuated interplanetary solar flare proton intensities of all energies above 10 MeV (with some short time delay both in rise time and decay). To a first approximation, these may also be considered omnidirectional and isotropic, probably to within 10-15%, when integrated over each proton flare event.

Predictions of solar flare proton fluxes at 1 AU are usually obtained as a function of mission duration τ and confidence level Q[10] on the basis of a probabilistic analysis using a modified type of Poisson statistics.[11] This analysis includes the distinction between "ordinary" (OR) and "anomalously large" (AL) events and the probability of occurrence of the latter. Both AL and OR event fluences are nonlinear functions of Q and τ. For these predictions, only high quality comprehensive satellite measurements (not ground observations) are being used, covering almost the entire 20th solar cycle, since spectral information can be obtained only by satellites. There have been indications that descriptions of the solar flare environment in interplanetary space (at 1 AU), derived from interpretations and extrapolations of ground-based measurements, have not been very accurate in terms of spectra.

It should be noted that the statistics cannot predict when an AL event will occur, only the probability that one will occur in a given length of time. And it must be remembered that a

Table 1 Trapped electron fluxes[a] (Model AE17-HI, circular orbit, inclination = 0 deg, altitude = 35,790 km, parking longitude = 160° W and 70 °W) (average, orbit integrated, omnidirectional, integral, daily intensities)

E (>MeV)	WORST CASE: $\phi_p = 160^oW$ (e/cm^2 day)	BEST CASE: $\phi_p = 70^oW$ (e/cm^2 day)
.1	1.878E 12	1.446E 12
.5	2.789E 11	1.769E 11
1.0	5.861E 10	3.018E 10
1.5	1.375E 10	6.243E 09
2.0	3.224E 09	1.292E 09
2.5	8.832E 08	2.800E 08
3.0	2.419E 08	6.069E 07
3.5	1.313E 08	2.716E 07
4.0	7.122E 07	1.215E 07
4.5	3.153E 07	4.443E 06
5.0	1.396E 07	1.624E 06
5.5	3.862E 06	3.749E 05
6.0	1.069E 06	6.070E 04
6.5	–	–
7.0	–	–

[a] These fluxes represent local time (LT) averaged values.

NOTE: The new outer zone electron model AE17 is an interim model that has replaced the older AE4 model. For energies above 1.5 MeV this interim model contains upper and lower limit values to account for the discrepancy between existing data sets. The AE17-HI favors Vampola's fit to the OV1-19 data, while the AE17-LO is more representative of all data sets presently available to NSSDC. The AE17 does not reflect solar cycle variations.

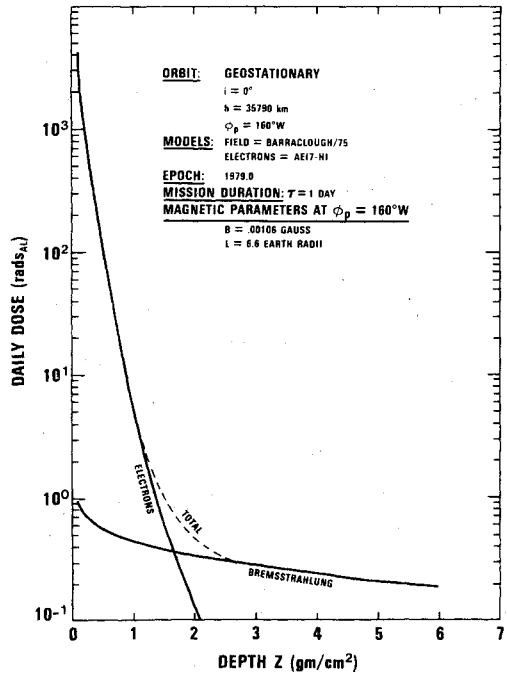

Fig. 8 Daily dose: worst case for geostationary orbit.

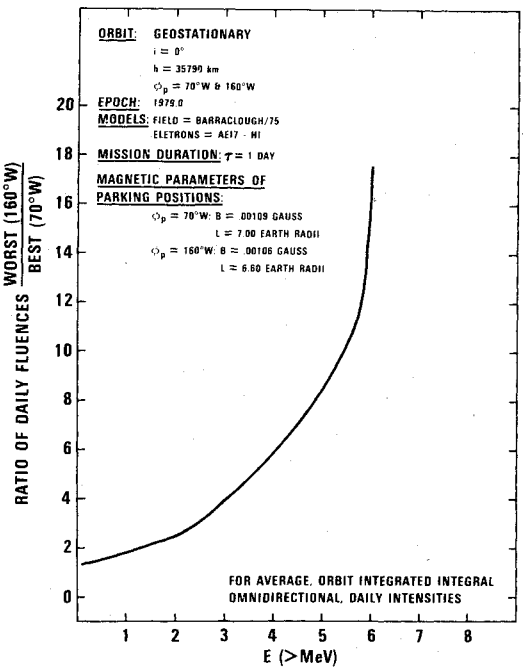

Fig. 7 Ratio of electron fluxes.

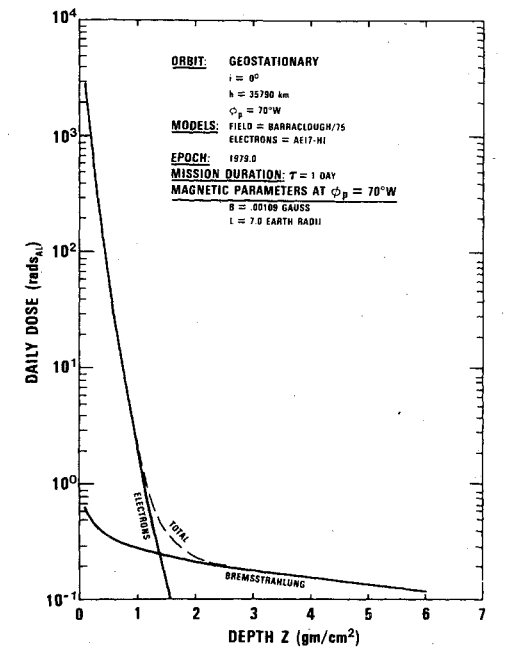

Fig. 9 Daily dose: best case for geostationary orbit.

single AL event will impart its total fluence within 2-4 days. Since AL-events are rare, small-sample statistics are the only appropriate prediction technique. This implies that for unmanned satellites with mission durations of $\tau \geq 1$ year, OR event fluences are not significant because probabilistic theory predicts the possible occurrence of at least *one* AL event, even for the lowest allowable confidence level ($Q = 80\%$). However, a different approach has to be followed if human presence in space is one's primary concern. Imagine, for example, the hypothetical case in which a space station is operated over a 6 year interval during the solar maximum activity phase with a crew rotation period of 90 days. This requires 24 crew changes. Now if one, three, or five AL events are predicted for that solar cycle (by any theory or method), all one can say is that 23, 21, or 19 crews will experience only OR event exposures over the short time interval of 90 days, while 1, 3, or 5 crews will be affected by the higher intensities of the AL event. Of course, this assumes that these 2-4 day events will fall entirely into one 90 day rotation period and that only one AL event will occur in that interval of time. Since nobody can predict exactly when an AL event will occur, each crew must be prepared for such an event.

As to OR event fluences, one can compute three guideline values: 1) select the most quiet 90 day period and obtain a total value, time integrated over the full 90 days (minimum); 2) repeat for the most active 90 day period (maximum); and 3) calculate a cycle mean for the entire 6-7 active years, excluding AL events (average).

Table 2 Electron and bremsstrahlung daily dose
(Model AEI7-HI, circular orbit, inclination = 0 deg, altitude = 35,790 km, parking longitudes = 160 °W and 70°W)

SHIELD THICKNESS (ALUMINUM)			BEST CASE: L = 7.0 Re			WORST CASE: L = 6.6 Re		
			PARKING LONGITUDE: 70°W			PARKING LONGITUDE: 160°W		
			ELECTRONS	BREMSSTRAHLUNG	TOTAL	ELECTRONS	BREMSSTRAHLUNG	TOTAL
Z (gm/cm^2)	t (mm)	t (mils)	($rads_{Al}$)	($rads_{Al}$)	($rads_{Al}$)	($rads_{Al}$)	($rads_{Al}$)	($rads_{Al}$)
.1	0.37	15	2.805E 03	6.060E-01	2.804E 03	4.356E 03	9.756E-01	4.359E 03
.2	0.74	29	8.307E 02	4.797E-01	8.312E 02	1.429E 03	7.625E-01	1.430E 03
.3	1.11	44	2.134E 02	4.216E-01	3.137E 02	5.879E 02	6.682E-01	5.885E 02
.4	1.48	58	1.308E 02	3.841E-01	1.312E 02	2.631E 02	6.079E-01	2.637E 02
.5	1.85	73	5.951E 01	3.567E-01	5.986E 01	1.267E 02	5.644E-01	1.272E 02
.6	2.22	87	2.841E 01	3.356E-01	2.874E 01	6.384E 01	5.304E-01	6.436E 01
.7	2.59	102	1.399E 01	3.181E-01	1.430E 01	3.326E 01	5.027E-01	3.375E 01
.8	2.96	117	7.047E 00	3.036E-01	7.351E 00	1.786E 01	4.795E-01	1.834E 01
.9	3.33	131	3.630E 00	2.910E-01	3.921E 00	9.890E 00	4.595E-01	1.035E 01
1.0	3.70	146	1.918E 00	2.800E-01	2.198E 00	5.663E 00	4.422E-01	6.107E 00
1.25	4.63	182	4.496E-01	2.574E-01	7.068E-01	1.664E 00	4.063E-01	2.071E 00
1.5	5.56	219	1.383E-01	2.396E-01	3.778E-01	6.351E-01	3.781E-01	1.013E 00
1.75	6.48	255	5.186E-02	2.250E-01	2.770E-01	2.825E-01	3.551E-01	6.375E-01
2.0	7.41	292	2.030E-02	2.127E-01	2.330E-01	1.274E-01	3.356E-01	4.630E-01
2.5	9.26	365	2.733E-03	1.926E-01	1.953E-01	2.254E-02	3.038E-01	3.263E-01
3.0	11.11	437	3.071E-04	1.765E-01	1.768E-01	3.504E-03	2.786E-01	2.822E-01
3.5	12.96	510	3.400E-05	1.632E-01	1.632E-01	5.595E-04	2.576E-01	2.582E-01
4.0	14.81	583	3.926E-06	1.517E-01	1.517E-01	9.271E-05	2.397E-01	2.398E-01
4.5	16.67	656	4.600E-07	1.417E-01	1.417E-01	1.542E-05	2.239E-01	2.239E-01
5.0	18.52	729	5.337E-08	1.328E-01	1.328E-01	2.517E-06	2.099E-01	2.100E-01
5.5	20.37	802	5.995E-09	1.247E-01	1.247E-01	3.959E-07	1.974E-01	1.974E-01
6.0	22.22	875	6.414E-10	1.174E-01	1.174E-01	5.948E-08	1.859E-01	1.859E-01

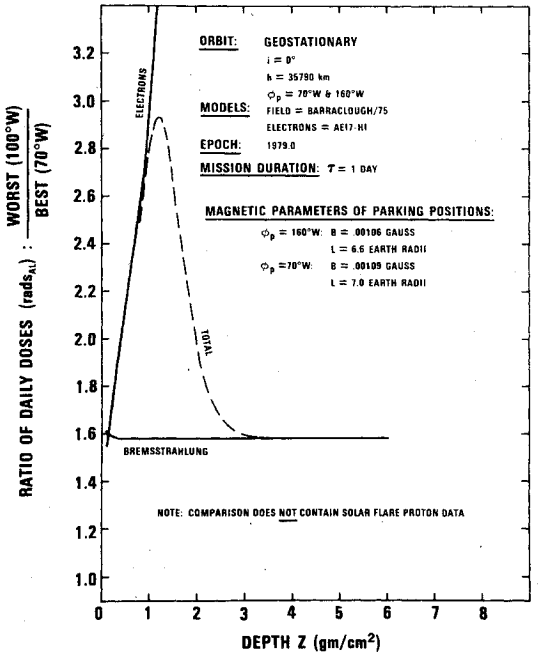

Fig. 10 Daily dose ratios.

Results of Orbital-Flux Integrations and Dose-Shielding Calculations

From the L trace in Fig. 3, the two absolute extrema (positions 70°W and 160°W) were selected for investigation. It is a fortuitous coincidence for several U.S. geostationary missions that the continental United States lies within the longitude range bounded by these two values.

Electrons

The AEI7-HI orbit integrated, omnidirectional, integral, daily electron fluxes are given in Table 1 for both parking positions. These are labeled "worst case" and "best case," corresponding to the L values of 6.6 and 7.0 Earth radii, respectively, since the time-averaged gradients are negative. The respective spectra are plotted in Fig. 6, and the ratios of worst-to-best fluxes are shown in Fig. 7, which also provides a measure of the radial dependence of the environment. Table 2 lists the daily electron, bremsstrahlung,† and total aluminum doses for the two injection longitudes, obtained from a simple two-dimensional, infinite slab geometry (2π steradian omnidirectional incidence). The same information is plotted in Figs. 8 and 9, while Fig. 10 shows the three ratios. It should be noted that the identical surface incident spectra will yield different dose-depth curves when used with other shield geometries (e.g., spherical). This is also true for protons.

It is evident that up to a shield thickness of about 1 g/cm^2 the primary electron dose prevails. Between 1 and 3 g/cm^2, the bremsstrahlung components become increasingly more significant: the constant bremsstrahlung ratio takes over and pulls the "total" curve down.

Trapped Protons

Similar to electrons, trapped proton data are also presented, in Table 3, in terms of AP8-MAX orbit integrated, omnidirectional, integral, daily fluxes, for "worst case" and "best case" parking longitudes.

Figure 11 shows the corresponding spectral plots and Fig. 12 gives the worst-to-best ratio curve.

†These are crude bremsstrahlung estimates, believed to be on the low side. They should be considered only qualitatively and they are being used for illumination purposes only. More exact calculations are in progress and will be reported in a subsequent paper.

Table 3 Trapped proton fluxes (Model AP8-MAX, circular orbit, inclination = 0 deg, altitude = 35,790 km, parking longitude = 160°W and 70°W) (average, orbit integrated, omnidirectional, integral, daily intensities)

E (>MeV)	WORST CASE: ϕ p = 160°W (p/cm^2 day)	BEST CASE: ϕp = 70°W (p/cm^2 day)
.01	2.365E 12	2.822E 11
.03	1.758E 12	2.144E 11
.05	1.307E 12	1.628E 11
.07	9.718E 11	1.237E 11
.10	6.230E 11	8.190E 10
.20	1.415E 11	2.072E 10
.30	5.651E 10	8.704E 09
.40	2.257E 10	3.656E 09
.50	9.015E 09	1.536E 09
.60	3.601E 09	6.452E 08
.70	1.424E 09	2.752E 08
.80	5.630E 08	1.174E 08
.90	2.226E 08	5.006E 07
1.00	8.802E 07	2.135E 07
1.25	8.654E 06	2.536E 06
1.50	8.507E 05	3.013E 05
1.75	–	–

NOTE: The new proton model AP8 has been issued in two versions, reflecting solar cycle variations (AP8-MAX, AP8-MIN). However, both yield identical results since no solar cycle changes of any consequence occur at the synchronous altitude regime.

The rapid drop-off of the spectra reflect the absence of medium-to-high-energy protons in the synchronous altitude regime. Here, too, as with the electrons, the ratios indicate the degree of radial dependence.

Dose calculations were not performed for these low-energy particles because they would be stopped by a shield even as thin as 1.5 mils of aluminum and such calculations would serve no practical purpose.

Solar Flare Protons

As previously indicated, the exposure of a geostationary spacecraft to solar flare protons is not dependent on the "parking longitude"; all geostationary positions are exposed to the fluxes observed outside the magnetosphere. However, it remains unresolved whether, during the increased activity phase of the solar cycle, a given mission will encounter only OR event fluences over a specified time interval, or whether the satellite may be inundated with energetic solar protons by the occurrence of an AL event in the same time interval. In that case, the OR event contributions become insignificant, as mentioned before.

Recognizing the distinction between manned and unmanned missions, probabilistic theory can provide some predictions to be made. Different criteria apply to these two categories of missions. Most unmanned geostationary projects are of multiyear duration (3, 5, or even 10 years). None are known to be planned for less than 1 year. On the other hand, manned missions are mostly planned for relatively short durations (up to about 90 days) on account of the human factor. Some implications of this difference in mission duration have been discussed in a preceding section. Of course, the radiation exposure of manned mission hardware systems and equipment, which remain in orbit for long periods of time (to be used by several subsequent crews), should be evaluated as a long duration mission.

To facilitate an evaluation of either manned or unmanned missions, both OR event and AL event data are presented for the conditions specified in Table 4. Table 5 lists the corresponding unattenuated, interplanetary, omnidirectional, integral solar flare proton fluences for OR events (90 day total) and for AL events (1 event). The total of both is given in the last column. These tabular data are plotted in Fig. 13. Table 6 gives the results of shielding and dose calculations for these fluences in an arrangement similar to that of Table 5. The corresponding dose-depth curves are shown in Fig. 14.

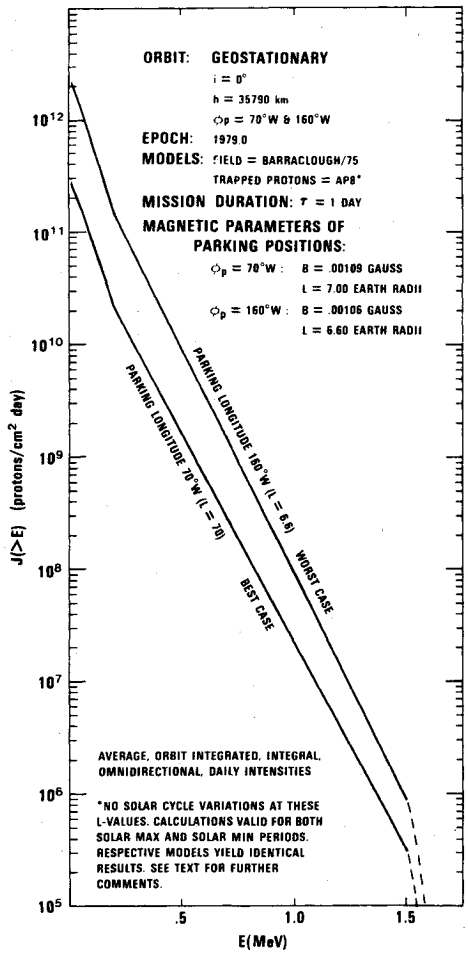

Fig. 11 Trapped proton fluxes.

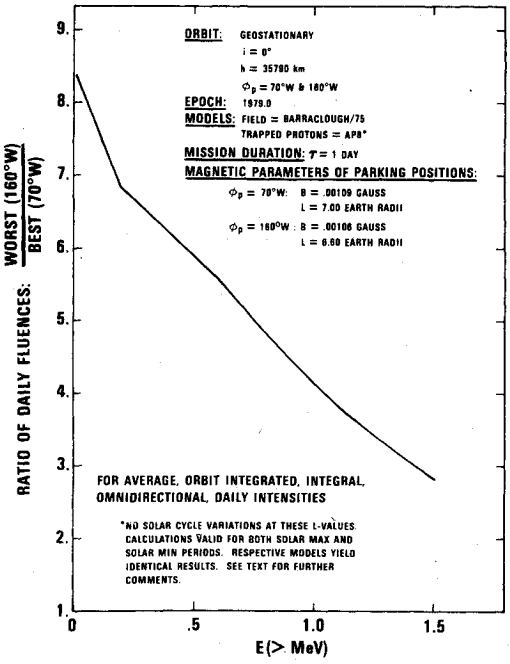

Fig. 12 Ratio of proton fluxes.

Table 4 Mission conditions pertaining to Tables 5 and 6

Event type	Confidence level Q, %	Mission duration τ	Predicted no. of events
OR	89	90 days	N.A.
AL	80	10-34 mos.	1
	85	7-27 mos.	1
	90	5-19 mos.	1
	95	2-12 mos.	1
	99	1-5 mos.	1

Table 5 Eneregetic solar flare protons (parking longitude: any) (unattenuated, interplanetary, omnidirectional, integral fluences)

E (>MeV)	OR[a] FLUENCES (p/cm^2)[c]	AL[b] FLUENCES (p/cm^2)[d]	TOTAL (p/cm^2)
10	4.842E 08	1.680E 10	1.728E 10
20	4.134E 08	1.152E 10	1.193E 10
30	3.530E 08	7.900E 09	8.253E 09
40	3.014E 08	5.417E 09	5.718E 09
50	2.574E 08	3.714E 09	3.971E 09
60	2.197E 08	2.547E 09	2.767E 09
70	1.876E 08	1.746E 09	1.934E 09
80	1.602E 08	1.197E 09	1.357E 09
90	1.368E 08	8.210E 08	9.578E 08
100	1.168E 08	5.629E 08	6.797E 08
	ENCOUNTERED IN 90-DAY PERIOD WHEN NO AL EVENT OCCURS		ENCOUNTERED IN 90-DAY PERIOD WHEN ONE AL EVENT OCCURS

Epoch: 1979
Models: Field = Barraclough/75
Solar flare protons = SOLPRO

a OR = ordinary event.
b AL = anomalously large event.
c Total fluences for $\tau = 90$ days.
d Total fluences for 1 AL event.

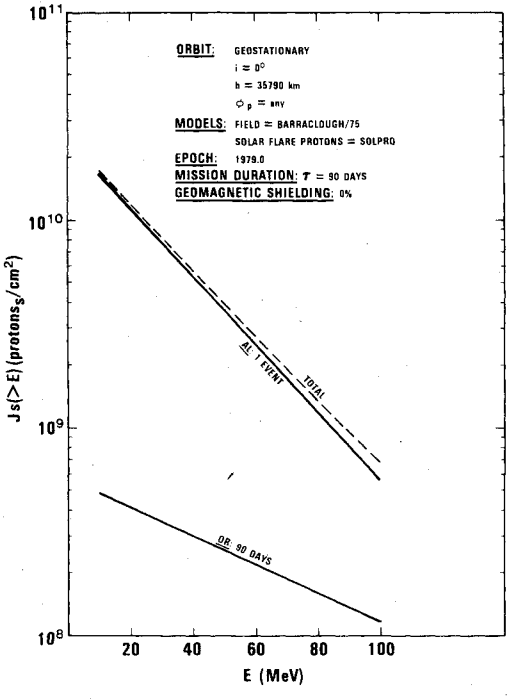

Fig. 13 Solar proton fluence.

Table 6 Energetic solar-flare-proton dose (parking longitude: any)

SHIELD THICKNESS (ALUMINUM) t (mm)	t (mils)	OR[a] DOSE (rads$_{AL}$)[c]	AL[b] DOSE (rads$_{AL}$)[d]	TOTAL DOSE (rads$_{AL}$)
.1	0.37	15	1.874E 01	1.102E 03	1.121E 03
.2	0.74	29	1.688E 01	9.379E 02	9.548E 02
.3	1.11	44	1.569E 01	8.307E 02	8.464E 02
.4	1.48	58	1.479E 01	7.503E 02	7.651E 02
.5	1.85	73	1.403E 01	6.843E 02	6.983E 02
.6	2.22	87	1.336E 01	6.268E 02	6.402E 02
.7	2.59	102	1.276E 01	5.767E 02	5.895E 02
.8	2.96	117	1.222E 01	5.336E 02	5.458E 02
.9	3.33	131	1.173E 01	4.955E 02	5.128E 02
1.0	3.70	146	1.128E 01	4.617E 02	4.730E 02
1.25	4.63	182	1.026E 01	3.897E 02	4.000E 02
1.50	5.56	219	9.391E 00	3.327E 02	3.421E 02
1.75	6.48	255	8.655E 00	2.875E 02	2.962E 02
2.0	7.41	292	8.017E 00	2.507E 02	2.587E 02
2.5	9.26	365	6.961E 00	1.947E 02	2.017E 02
3.0	11.11	437	6.125E 00	1.549E 02	1.610E 02
3.5	12.96	510	5.439E 00	1.254E 02	1.308E 02
4.0	14.81	583	4.862E 00	1.029E 02	1.078E 02
4.5	16.67	656	4.366E 00	8.535E 01	8.972E 01
5.0	18.52	729	3.930E 00	7.122E 01	7.515E 01
5.5	20.37	802	3.536E 00	5.956E 01	6.310E 01
6.0	22.22	875	3.181E 00	4.996E 01	5.314E 01
			ENCOUNTERED IN A 90-DAY PERIOD WHEN NO AL EVENT OCCURS		ENCOUNTERED IN A 90-DAY PERIOD WHEN ONE AL EVENT OCCURS

Epoch: 1979.0
Models: Field = Barraclough/75
Solar flare protons = SOLPRO

a OR = ordinary event.
b AL = anomalously large event.
c Dose for $\tau = 90$ days.
d Dose for 1 AL event.

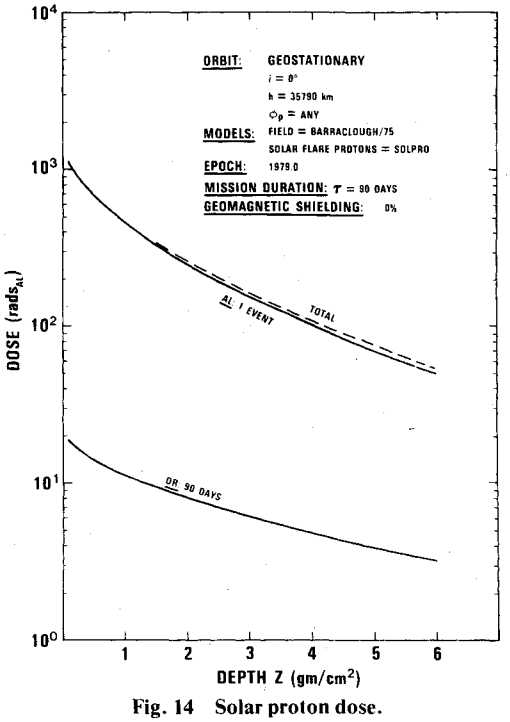

Fig. 14 Solar proton dose.

Discussion and Conclusions

In order to evaluate correctly the impact of the charged-particle radiation on geostationary missions, it is necessary to distinguish manned and unmanned types, because different needs exist and different criteria apply. The human presence in the former type predicates that the primary concern lies with radiation effects posing medical-biological hazards,

whereas in the latter type, mostly long-range degradation effects in materials are of concern. Note that instrument interference effects or measurement contamination has not be considered in this study.

For manned missions, the ambient electron population constitutes a definite health hazard for extravehicular activities (EVA), even though, for each crew member, these may be restricted to relatively brief time intervals, totaling maybe a few days over the short mission duration (not expected to exceed 90 days). The predicted flux levels and spectral distributions in the geostationary L range (6.6-7.0 Earth radii), however, are not severe enough to pose a threat for crew members in a well-shielded habitat or working area (≥ 3 g/cm^2). For example, behind a shield of 3 g/cm^2, the total 90 day dose from the primary incident electrons is insignificantly small: approximately 0.5 rads-aluminum for the worst case. This, of course, represents a surface (or skin) dose and a depth dose would be appropriately attenuated by the absorbing material itself. In comparison, the secondary bremsstrahlung contribution is nontrivial, amounting to about 16 and 25 rads-aluminum for the best and worst cases, respectively, for a 90 day total.

For unmanned missions, one has to consider at least an annual dose accumulation behind a nominal satellite skin. Satellite skin thicknesses vary widely, ranging from about 0.8 mm of equivalent aluminum to about 5.0 mm. Also, most radiation-sensitive spacecraft components are rarely placed directly under the satellite skin. They are in boxes that are usually mounted in the interior of the spacecraft, behind other equipment. This arrangement, evaluated three-dimensionally over 4π steradians, provides substantial additional shielding to the sensitive components. In order to obtain estimates, a reasonable total shield approximation would be about 0.7 g/cm^2 ($\sim$2.6 mm) of equivalent aluminum. Behind such a shield, the annual total electron and bremsstrahlung dose amounts to about 5.2×10^3 rads for the best geostationary position (70°W longitude) and to about 1.2×10^4 for the worst position (160°W longitude). It should be noted that only about 2% of these totals derive from bremsstrahlung. With these doses, the "softest" components should have no difficulty surviving at least one year in the synchronous environment. By providing increased shielding, either by geometry (rearranging on-board equipment) or by weight (using additional shielding), the lifetime of the most sensitive components could be substantially extended.

Trapped protons are of no consequence to either type of mission because of their very low energies. Conceivably, some interest in these particles may exist in areas of solar cell studies or in cases where surface effects on thermal coatings or experiment filters may be important.

Finally, in regards to solar flare protons, the average OR event 90 day total dose of about 6 rads is tolerably low for manned missions. For these missions the situation becomes very serious if an AL event should occur. It may give, within a couple of days, a skin dose of about 155 rads-aluminum to the crew, while in their shielded (≥ 3 g/cm^2) working area. The annual solar-flare-proton dose contributions to unmanned missions are relatively small. In comparison to the corresponding combined electron-bremsstrahlung dose, they amount to about 12% for the best position and about 5% for the worst position. The impact of high-charge cosmic rays (of galactic or solar origin) on geostationary missions will be the object of a subsequent study.

References

[1] McIlwain, C.E., "Coordinates for Mapping the Distribution of Magnetically Trapped Particles," *Journal of Geophysical Research,* Vol. 66, 1961, pp. 3681-3691.

[2] Singley, G.W. and Vette, J.I., "A Model Environment for Outer Zone Electrons," NSSDC 72-13, National Space Science Data Center, Greenbelt, Md., Dec. 1972.

[3] Chan, K.W., Teague, M.J., Schofield, N.J., and Vette, J.I., "Modeling of Electron Time Variations in the Radiation Belts," *American Geophysical Union* Geophysical Monograph 21, *Quantitative Modeling of Magnetospheric Processes,* June 1978.

[4] Singley, G.W. and Vette, J.I., "The AE4 Model of the Outer Radiation Zone Electron Environment," NSSDC 72-06, National Space Science Data Center, Greenbelt, Md., Aug. 1972.

[5] Teague, M.J., private communication, 1978.

[6] Sawyer, D.M. and Vette, J.I., "AP8 Trapped Proton Environment for Solar Maximum and Solar Minimum," NSSDC 76-06, National Space Science Data Center, Greenbelt, Md., Dec. 1976.

[7] King, J.H., "Models of the Trapped Radiation Environment, Volume IV: Low Energy Protons," NASA SP-3024, 1967.

[8] Lavine, J.P. and Vette, J.I., "Models of the Trapped Radiation Environment, Volume V: Inner Belt Protons," NASA SP-3024, 1969.

[9] Lavine, J.P. and Vette, J.I., "Models of the Trapped Radiation Environment, Volume VI: High Energy Protons," NASA SP-3024, 1970.

[10] Stassinopoulos, E.G., "SOLPRO: A Computer Code to Calculate Probabilistic Energetic Solar Proton Fluences," NSSDC 75-11, National Space Science Data Center, Greenbelt, Md., April 1975.

[11] King, J.H., "Solar Proton Fluences for 1977-1983 Space Missions," *Journal of Spacecraft and Rockets,* Vol. 11, June 1974, pp. 401-408.